EXIT-Chart Aided Code Design for Symbol-Based Entanglement-Assisted Classical Communication over Quantum Channels

Zunaira Babar, *Student Member, IEEE,* Soon Xin Ng, *Senior Member, IEEE,* and Lajos Hanzo, *Fellow, IEEE*
Communications, Signal Processing and Control Group, University of Southampton, Southampton, SO17 1BJ, U.K.
E-Mail: {zb2g10,sxn,lh}@ecs.soton.ac.uk

***Abstract*—Quantum-based transmission is an attractive solution conceived for achieving absolute security. In this quest, we have conceived an EXtrinsic Information Transfer (EXIT) chart aided channel code design for symbol-based entanglement-assisted classical communication over quantum depolarizing channels. Our proposed concatenated code design incorporates a Convolutional Code (CC), a symbol-based Unity Rate Code (URC) and a soft-decision aided 2-qubit Superdense Code (2SD), which is hence referred to as a CC-URC-2SD arrangement. We have optimized our design with the aid of non-binary EXIT charts. Our proposed design operates within 1 dB of the achievable capacity, providing attractive performance gains over its bit-based counterpart. Quantitatively, the bit-based scheme requires 60% more iterations than our symbol-based scheme for the sake of achieving perfect decoding convergence. Furthermore, we demonstrate that the decoding complexity can be reduced by using memory-2 and memory-3 convolutional codes, while still outperforming the bit-based approach.**

Keywords*—*Entanglement-Assisted Classical Communication, Superdense Coding, Non-Binary EXIT Charts, Iterative Decoding.

I. Introduction

Quantum-based communication constitutes an attractive solution for absolute secure transmission [1]. More explicitly, any 'measurement' or 'observation' of the transmitted qubits by the eavesdropper destroys the associated quantum entanglement, hence instantly intimating the parties concerned [1]. In this context, entanglement-assisted transmission of classical information over quantum channels is of particular significance. This idea was conceived by Bennett [2] in his widely-cited 2-qubit Superdense (2SD) coding protocol, which transmits 2 classical bits per channel use (cbits/use) of a noiseless quantum channel with the aid of a pre-shared maximally entangled qubit. The corresponding Entanglement-Assisted Classical Capacity (EACC) of the so-called quantum depolarizing channel was quantified in [3], [4]. Analogous to Shannon's well-known capacity theorem conceived for classical channels, EACC quantifies the capacity limit of reliable transmission of classical information over a noisy quantum channel, when an unlimited amount of noiseless entanglement is shared between the transmitter and the receiver.

Recently, Chiuri *et al.* [5] experimentally demonstrated the achievable entanglement-assisted classical capacity of a quantum depolarizing channel, which paves the way for the practical implementation of future quantum-based communication systems. However, reliable transmission over quantum systems is impossible without efficient error correction codes. In our prior research [6], we exploited the efficient near-capacity classical code designs of [7]–[9] for designing a bit-based concatenated code operating close to the bit-based EACC of the quantum depolarizing channel. More explicitly, the code design presented in [6] incorporates an Irregular Convolutional Code (IRCC), a symbol-based Unity Rate Code (URC) and a soft-decision aided Superdense Code (SD), which is hence referred to as an IRCC-URC-2SD arrangement, when 2SD is used. Since the design of [6] uses a bit interleaver and hence bit-based iterative decoding, symbol-to-bit conversion is invoked before the related soft-information is fed from the inner decoder (URC-SD) to the outer decoder (IRCC). This in turn incurs an inherent capacity loss, which cannot be recovered by the bit-based coding scheme of [6]. This capacity loss was previously identified in [10] for classical discrete-memoryless channels and a modified binary LDPC code was proposed to circumvent this issue. By contrast, in this paper we have conceived an iterative code design for symbol-based CC-URC-2SD to overcome the capacity loss. Our proposed design incorporates a single Convolutional Code (CC) as the outer component, while the URC and 2SD schemes constitute the amalgamated inner code. We have optimized our design with the aid of non-binary EXtrinsic Information Transfer (EXIT) charts of [7]–[9]. Our simulation results demonstrate that, despite its lower encoding/decoding complexity, the symbol-based CC-URC-2SD provides a significant Bit-Error-Rate (BER) performance improvement over the bit-based IRCC-URC-2SD. Quantitatively, after 2 iterations, our proposed design incorporating a memory-4 CC outperforms the IRCC-URC-2SD scheme of [6] by 3.7 dB at a BER of 10^{-4}. Furthermore, the IRCC-URC-2SD arrangement of [6] requires around 60% more iterations than the CC-URC-2SD for achieving perfect decoding convergence. We also demonstrate that the decoding complexity can be further reduced by using memory-2 and memory-3 convolutional codes, which rely on only 4 and 8 states, respectively, per iteration.

This paper is organized as follows. We commence with a comparison of the symbol-based and bit-based EACC in Section II. Our system model will be presented in Section III, while the EXIT-chart aided design will be detailed in Section IV. Finally, our results will be discussed in Section V and our conclusions are offered in Section VI.

The financial support of the European Union under the auspices of the CONCERTO project, as well as that of the European Research Council under its Advanced Fellow grant is gratefully acknowledged.

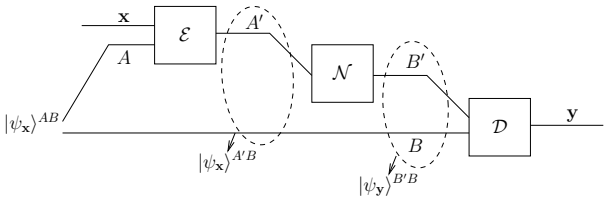

Fig. 1. Classical-quantum-classical transmission model employing 2SD.

II. Symbol-based Versus Bit-based Entanglement-Assisted Classical Capacity

The classical-quantum-classical transmission model, whereby classical information is transmitted over a quantum channel with the aid of superdense coding protocol [2], is depicted in Fig. 1. Here, Alice intends to transmit her 2-bit classical message $\mathbf{x}$ to Bob using a 2-qubit maximally entangled state $|\psi_{\mathbf{x}}\rangle^{AB} = \frac{1}{\sqrt{2}}\left(|0^A 0^B\rangle + |1^A 1^B\rangle\right)$, where A denotes the information qubit, while B is a pre-shared entangled qubit transmitted over a noiseless quantum channel. The classical message $\mathbf{x}$ is encoded by the block $\mathcal{E}$ of Fig. 1 into the corresponding quantum state using the 2SD coding protocol of [2]. The processed qubit A' is passed through a quantum depolarizing channel[1], which is denoted as $\mathcal{N}^{A'\to B'}$. Here, $\mathcal{N}^{A'\to B'}$ can be viewed as a Completely Positive Trace-Preserving (CPTP) mapping, which maps a state ρ onto a linear combination of itself and of the maximally entangled state. More explicitly, for a depolarizing probability p, this mapping is given by [1]:

$$\mathcal{N}_p(\rho) = (1-p)\rho + \frac{p}{3}\mathbf{X}\rho\mathbf{X} + \frac{p}{3}\mathbf{Y}\rho\mathbf{Y} + \frac{p}{3}\mathbf{Z}\rho\mathbf{Z}, \quad (1)$$

where $\mathbf{X}$, $\mathbf{Y}$ and $\mathbf{Z}$ are Pauli matrices. Therefore, a depolarizing channel characterized by the probability p inflicts either a bit flip ($\mathbf{X}$), a phase flip ($\mathbf{Z}$) or both ($\mathbf{Y}$) on the transmitted qubit with a probability of $p/3$.

The receiver Bob performs symbol-by-symbol Bell-basis measurement [1], [12] on the received state $|\psi_{\mathbf{y}}\rangle^{B'B}$ in block $\mathcal{D}$ of Fig. 1, which yields the 2-bit classical message $\mathbf{y}$. Thus, the overall transmission model reduces to a classical discrete-memoryless channel. Consequently, the i^{th} bit of $\mathbf{x}$ is related to that of $\mathbf{y}$ as follows:

$$y_i = x_i \oplus e_i \quad \text{or} \quad e_i = y_i \oplus x_i, \quad (2)$$

where $\oplus$ denotes modulo-2 addition and $\mathbf{e}$ can be viewed as the 2-bit classical equivalent of the quantum error encountered during transmission over the depolarizing channel characterized in Eq. (1). More specifically, the channel transition probabilities of the induced classical channel are given by:

$$P(\mathbf{y}|\mathbf{x} = \mathbf{x}^{(m)}) = \begin{cases} 1-p, & \text{if } E = 0 \\ p/3, & \text{if } E \in \{1,2,3\}, \end{cases} \quad (3)$$

where $\mathbf{x}^{(m)}$ is the hypothetically transmitted m^{th} symbol for $m \in \{0,1,2,3\}$ and E is the decimal equivalent of the 2-bit classical error $\mathbf{e}$ of Eq. (2). The resultant entanglement-assisted classical capacity is quantified as follows [3]:

$$C_{2sd} = 2 + (1-p)\log_2(1-p) + p\log_2(p/3) \text{ cbits/use}. \quad (4)$$

[1]A quantum channel can be used for modeling imperfections in quantum hardware as well as quantum-state flips imposed by the transmission medium, including free-space wireless channels and optical fiber links, when qubits are transmitted across these media [11].

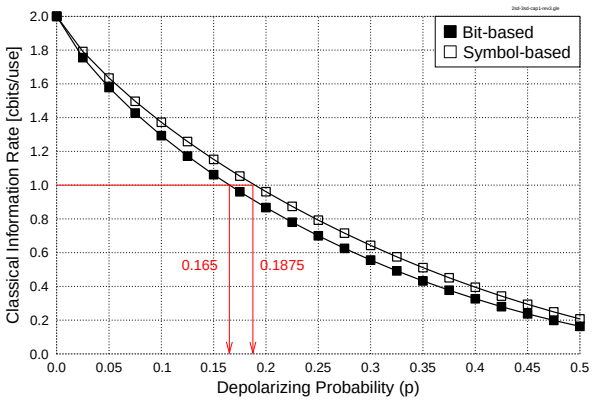

Fig. 2. Classical information rate (cbits/use) versus quantum depolarizing probability for 2SD.

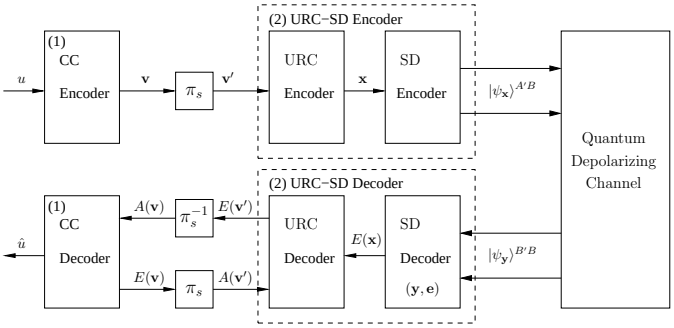

Fig. 3. Schematic of the proposed symbol-based CC-URC-2SD classical-quantum communication system.

The corresponding bit-based capacity may be computed by marginalizing the symbol-based channel transition probabilities $P(\mathbf{y}|\mathbf{x})$ of Eq. (3) to the bit-based probabilities $P(y_i|x_i)$ for $i \in \{0,1\}$, assuming that the constituent bits are independent [6]. More specifically, we get:

$$P(y_i = x_i|x_i) = 1 - \frac{2}{3}p, \quad P(y_i \neq x_i|x_i) = \frac{2}{3}p, \quad (5)$$

and the symbol-based capacity of Eq. (4) is reduced to:

$$C_{2sd}^{\text{bit}} = 2 \times \left[1 + (1-\frac{2}{3}p)\log_2(1-\frac{2}{3}p) + \frac{2}{3}p\log_2(\frac{2}{3}p)\right]. \quad (6)$$

The corresponding capacity loss for the bit-based 2SD scheme is depicted in Fig. 2, which compares the bit-based and symbol-based capacities of Eq. (4) and Eq. (6), respectively. As gleaned from Fig. 2, for a classical information rate of 1 cbit/use, a bit-based system ensures reliable transmission for $p \leq 0.165$, while a symbol-based system would increase the noise limit to $p = 0.1875$. Therefore, a bit-based error correction scheme, which ignores the correlation between the bits, incurs an inherent irrecoverable capacity loss of around 0.6 dB[2] as compared to its symbol-based counterpart.

III. System Model

Fig. 3 shows the proposed system model. At the transmitter, the system is fed with classical bits $\{u\}$, which are encoded by a $1/2$-rate Convolutional Code (CC). The encoded 4-ary coded symbols $\mathbf{v} = [v_0, v_1]$ are then interleaved by a symbol

[2]The difference in dB between two channel depolarizing probabilities p_1 and p_2 is calculated as follows [6], [11], [13]: $\left(10 \times \log_{10}\frac{p_1}{p_2}\right)$.

interleaver (π_s), yielding the permuted symbol stream $\mathbf{v}'$, which is fed to the symbol-based recursive Unity Rate Code (URC) having a generator polynomial of $G(D) = \frac{1}{1+D}$ [8]. It must be pointed out here that URC is used as a precoder having an Infinite Impulse Response (IIR), which is invoked for the sake of efficiently spreading the extrinsic information without increasing the system's delay. This allows the inner decoder component to have an EXIT curve reaching the $(1, 1)$ point of perfect decoding convergence to a vanishingly low BER, as detailed in [14]. Then classical to quantum domain conversion then takes place at the SD encoder of Fig. 3, which maps the classical symbols $\mathbf{x}$ onto the orthogonal quantum states $|\psi_{\mathbf{x}}\rangle^{A'B}$ using the maximally entangled state $|\psi_{\mathbf{x}}\rangle^{AB}$, as discussed in Section II. Hence, the SD encoder has a function similar to that of the classical PSK/QAM bit-to-symbol mapper, which maps several classical bits onto a complex-valued phasor for communication using the classical electromagnetic waves. Since the resultant system of Fig. 3 has three serially concatenated stages, we simplify it by intrinsically amalgamating our Superdense code (SD) with the symbol-based URC, which hence constitutes an amalgamated inner component, while the CC is our outer component.

The encoded qubits $|\psi_{\mathbf{x}}\rangle^{A'B}$ are serially transmitted over the quantum depolarizing channel. Recall from Fig. 1 that the processed qubit A' is transmitted over the noisy quantum channel, while B is shared between Alice and Bob over a noiseless quantum channel. At the receiver, the SD decoder of Fig. 3 performs symbol-by-symbol Bell-basis measurement on the received orthogonal states $|\psi_{\mathbf{y}}\rangle^{B'B}$, yielding the classical symbols $\mathbf{y}$. Furthermore, in contrast to the conventional SD decoder, which generates the hard-decision outputs, we use the SD decoder of [6], which computes the extrinsic probability $E(\mathbf{x})$ for the transmitted classical symbol $\mathbf{x}$, as follows:

$$E(\mathbf{x}) \approx P(\mathbf{y}|\mathbf{x}), \tag{7}$$

where $P(\mathbf{y}|\mathbf{x})$ is given by Eq. (3). The soft output $E(\mathbf{x})$ is then fed to the URC MAP decoder, which engages in iterative decoding with the CC decoder, as depicted in Fig. 3. Here the notations $A(\mathbf{b})$ and $E(\mathbf{b})$ refer to the *a priori* and *extrinsic* probabilities of $\mathbf{b}$, where we have $\mathbf{b} \in \{\mathbf{x}, \mathbf{v}, \mathbf{v}'\}$, which are exploited for achieving decoding convergence to a vanishingly low BER.

IV. Non-Binary EXIT-Chart Aided Code Design

EXIT charts [8], [9], [15] are capable of visualizing the convergence behaviour of iterative decoding schemes by exploiting the input/output relations of the constituent decoders in terms of their average Mutual Information (MI) transfer characteristics. Since our proposed model of Fig. 3 relies on symbol-based iterative decoding, we invoke non-binary EXIT chart of [7]–[9], which visualizes the exchange of the following four MI terms - average *a priori* MI between $\mathbf{v}'$ and $A(\mathbf{v}')$: $I_{A(\mathbf{v}')}$, average *a priori* MI between $\mathbf{v}$ and $A(\mathbf{v})$: $I_{A(\mathbf{v})}$, average *extrinsic* MI between $\mathbf{v}'$ and $E(\mathbf{v}')$: $I_{E(\mathbf{v}')}$, and average *extrinsic* MI between $\mathbf{v}$ and $E(\mathbf{v})$: $I_{E(\mathbf{v})}$. Here, $I_{A(\mathbf{v}')}$ and $I_{E(\mathbf{v}')}$ constitute the EXIT curve of the inner decoder, while $I_{A(\mathbf{v})}$ and $I_{E(\mathbf{v})}$ yield the EXIT curve of the outer decoder. For the sake of constructing the inner and outer EXIT curves, the *a priori* information, $A(\mathbf{v}')$ and $A(\mathbf{v})$ respectively, is modeled for a range of $I_{A(\mathbf{v}')}, I_{A(\mathbf{v})} \in [0, 1]$[3]. The underlying *a priori* channel is modeled using a Gaussian distribution, which has a mean of zero and a variance of σ_A^2, assuming that the constituent bits of the 4-ary symbol are independent. The corresponding average *extrinsic* MI can be formulated as [7], [16]:

$$I_{E(\mathbf{b})} = \log_2 M + \mathrm{E}\left[\sum_{m=0}^{M-1} E(\mathbf{b}^{(m)}) \log_2(E(\mathbf{b}^{(m)}))\right], \tag{8}$$

where we have $\mathbf{b} \in \{\mathbf{v}, \mathbf{v}'\}$, while $M = 4$ and $m \in \{0, 3\}$. Furthermore, E[.] denotes the expectation (or time average) operation. The resultant inner decoder EXIT function $T_{\mathbf{v}'}$ and the corresponding outer decoder EXIT function $T_{\mathbf{v}}$ are given by:

$$I_{E(\mathbf{v}')} = T_{\mathbf{v}'}[I_{A(\mathbf{v}')}, p], \quad I_{E(\mathbf{v})} = T_{\mathbf{v}}[I_{A(\mathbf{v})}]. \tag{9}$$

More explicitly, unlike $T_{\mathbf{v}}$, $T_{\mathbf{v}'}$ is a function of the depolarizing probability p, since the inner decoder depends on the channel output. Finally, the MI transfer characteristics of both the decoders encapsulated by $T_{\mathbf{v}'}$ and $T_{\mathbf{v}}$ are plotted in the same graph, with the x and y axes of the outer decoder swapped. The resultant EXIT chart is capable of visualizing the exchange of extrinsic MI as a stair-case-shaped decoding trajectory, as the iterations proceed.

We have exploited the area property of EXIT charts [17] for optimizing our code design[4]. According to this property, the area under the EXIT curve of the inner decoder is approximately equal to the attainable channel capacity [17], provided that the channel's input symbols are equiprobable. Since our system model of Fig. 3 transmits classical information over a quantum depolarizing channel, the attainable channel capacity of the system is the entanglement-assisted classical capacity of Eq. (4). Furthermore, the area under the EXIT curve of the outer decoder is equivalent to $(1 - R_o)$, where R_o is its coding rate [17]. Therefore, our design objective is to find the optimal outer code[5] $\mathcal{C}$ having a coding rate R_o, which gives the best curve-shape match with the given inner decoder's EXIT curve. As a result, we have a marginally open tunnel between the EXIT curves of the inner and outer decoders at the highest possible depolarizing probability, which corresponds to the lowest possible SNR for a classical channel. The smaller the area within the EXIT tunnel, the closer the system's performance to the achievable channel capacity, but this is achieved at the cost of requiring more decoding iterations for achieving decoding convergence to an infinitesimally low BER.

V. Results and Discussions

Using the aforementioned non-binary EXIT-chart aided design criterion, we have optimized our iterative code structure of Fig. 3 to design a system with a coding rate of 1 cbit/use. According to the symbol-based capacity curve of Fig. 2,

[3]For non-binary symbols, mutual information can be greater than 1, i.e. $I_{A(\mathbf{v}')}, I_{A(\mathbf{v})} \in [0, 2]$ for our case in this paper. However, we have normalized the mutual information to unity for simplicity.

[4]The area property was proved only for Binary Erasure Channel (BEC) in [17]. However, it has been extensively used for designing near-capacity codes even when the *a priori* channel is assumed to be Additive White Gaussian Noise (AWGN) [8].

[5]In the context of our paper, 'optimal code' means 'the best possible code'.

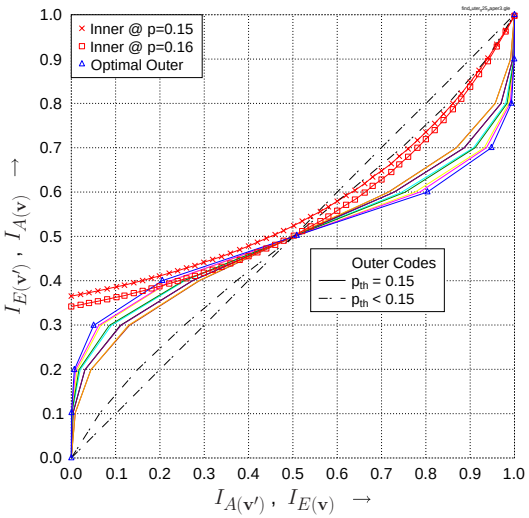

Fig. 4. Normalized EXIT curves of the CC-URC-2SD system. Various $1/2$-rate memory-4 convolutional codes were used as outer components. The optimal outer code has generator polynomials $(g_1, g_2) = (31, 36)_8$.

the corresponding maximum tolerable channel depolarizing probability for our system is $p = 0.1875$.

Design Objective I: For the sake of comparing the symbol-based scheme of Fig. 3 with the bit-based scheme of [6], which uses a $1/2$-rate memory-4 IRCC, find the optimal $1/2$-rate memory-4 convolutional code, which gives the best match with URC-2SD in the CC-URC-2SD configuration, when symbol-based iterative decoding is invoked.

For the sake of achieving this objective, we created the EXIT curves of all the possible $1/2$-rate memory-4 convolutional codes by evaluating all legitimate generator polynomials to find the optimal code $\mathcal{C}$, which yields a marginally open tunnel at the highest possible channel depolarizing probability. The EXIT characteristics of some of these $(2, 1, 4)$ CCs are plotted in Fig. 4 along with the inner decoder EXIT curve of the URC-2SD scheme at $p = 0.15$ and $p = 0.16$. As gleaned from the figure, all outer decoder EXIT curves plotted in 'solid' lines exhibit a convergence threshold of $p_{\text{th}} = 0.15$, i.e. a marginally open tunnel exists for $p = 0.15$. If the depolarizing probability is increased beyond 0.15, the inner and outer decoder EXIT curves will crossover, thereby closing the tunnel. By contrast, the pair of outer decoder EXIT curves plotted in 'dashed' lines have $p_{\text{th}} < 0.15$. Hence, our desired optimal code $\mathcal{C}$ is one of those associated with $p_{\text{th}} = 0.15$. It may be further observed in Fig. 4 that the EXIT curve labeled as 'Optimal Outer', whose octally represented generator polynomials are $(g_1, g_2) = (31, 36)_8$, converges faster than the others[6]. Therefore, we have selected it as our optimal outer component. The corresponding BER performance recorded for an interleaver length of $30,000$ symbols is plotted in Fig. 5. As it can be observed, the turbo-cliff formulation starts around $p = 0.15$, which matches the convergence threshold predicted using EXIT charts. More specifically, at $p \leq 0.15$, the system converges to a low BER as the number of iterations increases, while for $p \geq 0.16$, the performance fails to improve upon increasing the number

[6]The optimal outer code yields the widest area between the inner and outer EXIT curves after the $(0.5, 0.5)$-point. This signifies that less decoding iterations are required.

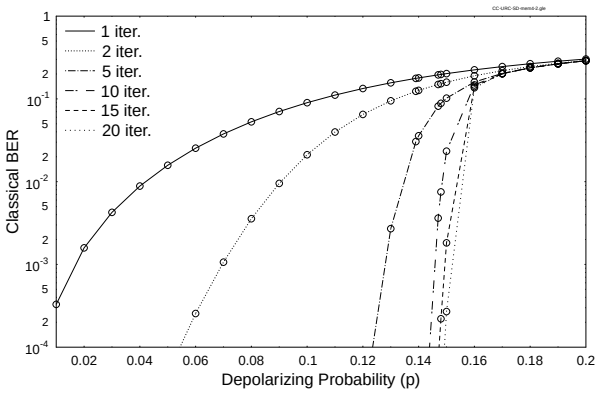

Fig. 5. The BER versus quantum depolarizing probability for CC-URC-SD system with CC$(2, 1, 4)$, having generator polynomials $(g_1, g_2) = (31, 36)_8$, as the outer component. *Interleaver length* $= 30,000$ *symbols.*

of iterations. This is because, as shown in Fig. 4, the EXIT chart tunnel closes at $p = 0.16$. Thus, the system fails to converge to a low BER for $p \geq 0.16$. It may also be observed that performance only moderately improves with diminishing returns at higher number of iterations. Furthermore, since doubling the number of iterations from 10 to 20 only improves the performance slightly at a BER of 10^{-4}, we may conclude that 20 iterations are sufficient to reach the $(1, 1)$-point of near-perfect convergence.

We further compare our symbol-based CC-URC-2SD with the bit-based IRCC-URC-2SD of [6] in Fig. 6, where the uncoded BER of 2SD is also plotted. It may be observed that both systems have the same convergence threshold of $p = 0.15$, which is within $[10 \times \log_{10}(\frac{0.15}{0.1875})] = 1$ dB of the achievable noise limit. Since an IRCC has a higher encoding and decoding complexity than a single-component CC, we can achieve the same convergence threshold at a lower encoding/decoding complexity using the symbol-based scheme. Furthermore, the CC-URC-2SD system exhibits an improved BER performance compared to the IRCC-URC-2SD scheme, as shown in Fig. 6. After 2 iterations, the IRCC-URC-2SD arrangement yields a BER of 10^{-4} at $p = 0.0225$, while CC-URC-SD scheme has a BER of 10^{-4} at $p = 0.0525$. Therefore, CC-URC-2SD outperforms the IRCC-URC-2SD arrangement by $[10 \times \log_{10}(\frac{0.0225}{0.0525})] = 3.7$ dB. Moreover, as demonstrated in [6], the IRCC-URC-2SD scheme achieves perfect convergence in around 32 iterations, while only 20 iterations are sufficient for the symbol-based CC-URC-2SD. We further benchmark the performance against the achievable symbol-based capacity of $p = 0.1875$. At a BER of 10^{-4} and after a sufficiently high number of iterations (20 for CC-URC-2SD and 32 for IRCC-URC-2SD), the CC-URC-2SD scheme operates within $[10 \times \log_{10}(\frac{0.149}{0.1875})] = 1$ dB of the capacity, while the IRCC-URC-2SD regime exhibits a deviation of $[10 \times \log_{10}(\frac{0.142}{0.1875})] = 1.2$ dB from the capacity. Thus, the performance of both systems is comparable once perfect convergence is achieved. However, the IRCC-URC-2SD scheme requires 60% more iterations than the symbol-based CC-URC-SD arrangement.

Design Objective II: Find the optimal $1/2$-rate memory-2 and memory-3 convolutional codes, which exhibit the best EXIT-curve shape match with URC-2SD in the CC-URC-2SD configuration, when symbol-based iterative decoding is invoked.

Again, for the sake of finding the optimal memory-2 and

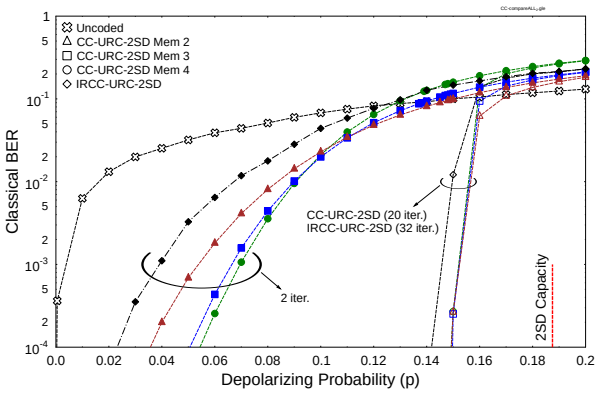

Fig. 6. Comparison of the BER performance curves for the bit-based IRCC-URC-2SD of [6] and the symbol-based CC-URC-2SD design with varying constraint length.

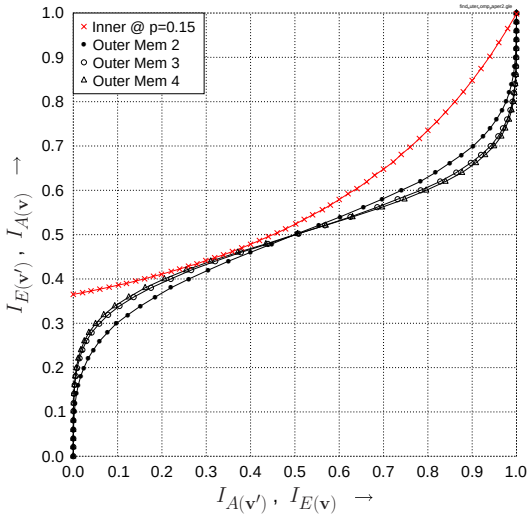

Fig. 7. Normalized EXIT curves of the CC-URC-2SD system with varying outer components. Optimal outer components are: CC$(2, 1, 2)$ with generator polynomials $(g_1, g_2) = (7, 5)_8$, CC$(2, 1, 3)$ with generator polynomials $(g_1, g_2) = (17, 15)_8$ and CC$(2, 1, 4)$ with generator polynomials $(g_1, g_2) = (31, 36)_8$.

memory-3 outer components, we created the EXIT curves for all the possible codes, as in Fig. 4. It was found that the CC$(2, 1, 2)$ having the generators $(g_1, g_2) = (7, 5)_8$ and the CC$(2, 1, 3)$ with generators $(g_1, g_2) = (17, 15)_8$ yield the best match. The corresponding EXIT curves are plotted in Fig. 7. All codes have the same decoding convergence threshold. The corresponding BER performance is compared in Fig. 6 after both 2 and 20 iterations. The CC associated with a higher constraint length exhibits a lower BER before perfect convergence is achieved, e.g. after 2 iterations as shown in Fig. 6. It also has to be noted here that all the three symbol-based configurations outperform the bit-based IRCC-URC-SD scheme. Furthermore, after 20 iterations, all codes have a similar performance at a BER of 10^{-4}. Codes having a lower constraint length have the additional benefit of a lower decoding complexity, since fewer states are invoked per iteration.

VI. Conclusions

In this paper, we have proposed an iterative code design for symbol-based entanglement-assisted classical communication over quantum depolarizing channels, which is optimized by exploiting non-binary EXIT charts. It was demonstrated that our proposed symbol-based scheme provides attractive performance gains over its bit-based counterpart. Moreover, we also investigated the impact of using convolutional codes with lower constraint lengths (i.e. memory 2 and 3), thereby reducing the decoding complexity by invoking fewer trellis states per iteration.

References

[1] M. A. Nielsen and I. L. Chuang, *Quantum Computation and Quantum Information*. Cambridge University Press, 2000.

[2] C. H. Bennett, "Communication via one- and two-particle operators on Einstein-Podolsky-Rosen states," *Physical Review Letters*, vol. 69, no. 20, p. 2881, 1992. [Online]. Available: http://dx.doi.org/%7B10.1103/PhysRevLett.69.2881%7D

[3] C. H. Bennett, P. W. Shor, J. A. Smolin, and A. V. Thapliyal, "Entanglement-assisted classical capacity of noisy quantum channels," *Phys. Rev. Lett.*, vol. 83, pp. 3081–3084, Oct 1999. [Online]. Available: http://link.aps.org/doi/10.1103/PhysRevLett.83.3081

[4] A. Holevo, "On entanglement-assisted classical capacity," *J. Math. Phys.*, vol. 43, no. 9, pp. 4326–4333, 2002.

[5] A. Chiuri, S. Giacomini, C. Macchiavello, and P. Mataloni, "Experimental achievement of the entanglement-assisted capacity for the depolarizing channel," *Phys. Rev. A*, vol. 87, p. 022333, Feb 2013. [Online]. Available: http://link.aps.org/doi/10.1103/PhysRevA.87.022333

[6] Z. Babar, S. X. Ng, and L. Hanzo, "Near-capacity code design for entanglement-assisted classical communication over quantum depolarizing channels," *IEEE Transactions on Communications*, vol. 61, no. 12, pp. 4801–4807, December 2013.

[7] J. Kliewer, S. X. Ng, and L. Hanzo, "Efficient computation of EXIT functions for non-binary iterative decoding," *IEEE Transactions on Communications*, vol. 54, no. 12, pp. 2133–2136, December 2006.

[8] L. Hanzo, T. H. Liew, B. L. Yeap, R. Y. S. Tee and S. X. Ng, *Turbo Coding, Turbo Equalisation and Space-Time Coding: EXIT-Chart-Aided Near-Capacity Designs for Wireless Channels, 2nd Edition*. New York, USA: John Wiley IEEE Press, March 2011.

[9] M. El-Hajjar and L. Hanzo, "EXIT charts for system design and analysis," *IEEE Communications Surveys Tutorials*, pp. 1–27, 2013.

[10] C. Weidmann and G. Lechner, "A fresh look at coding for q - ary symmetric channels," *IEEE Transactions on Information Theory*, vol. 58, no. 11, pp. 6959–6967, Nov 2012.

[11] Z. Babar, S. X. Ng, and L. Hanzo, "EXIT-chart aided near-capacity quantum turbo code design," *IEEE Transactions on Vehicular Technology (Accepted)*, 2014. [Online]. Available: http://eprints.soton.ac.uk/352606/

[12] P. Botsinis, S. X. Ng, and L. Hanzo, "Quantum search algorithms, quantum wireless, and a low-complexity maximum likelihood iterative quantum multi-user detector design," *IEEE Access*, vol. 1, pp. 94–122, 2013, http://ieeexplore.ieee.org/xpl/articleDetails.jsp?arnumber=6515077.

[13] M. M. Wilde and M.-H. Hsieh, "Entanglement boosts quantum turbo codes," in *IEEE International Symposium on Information Theory Proceedings (ISIT)*, Aug. 2011, pp. 445 – 449.

[14] K. R. Narayanan, "Effect of precoding on the convergence of turbo equalization for partial response channels," *IEEE Journal on Selected Areas in Communications*, vol. 19, no. 4, pp. 686–698, April 2001.

[15] S. ten Brink, "Convergence behaviour of iteratively decoded parallel concatenated codes," *IEEE Transactions on Communications*, vol. 49, no. 10, pp. 1727–1737, October 2001.

[16] S. X. Ng, O. Alamri, Y. Li, J. Kliewer, and L. Hanzo, "Near-capacity turbo trellis coded modulation design based on EXIT charts and union bounds," *IEEE Transactions on Communications*, vol. 56, no. 12, pp. 2030 –2039, december 2008.

[17] A. Ashikhmin, G. Kramer, and S. ten Brink, "Extrinsic information transfer functions: model and erasure channel properties," *IEEE Transactions on Information Theory*, vol. 50, no. 11, pp. 2657– 2673, November 2004.